sustainability

MDPI

Article

Dynamics of Zinder's Urban Landscape: Implications for Sustainable Land Use Management and Environmental Conservation

Kadiza Doulay Seydou [1,*], Wole Morenikeji [2], Abdoulaye Diouf [3], Kagou Dicko [1], Elbek Erdanaev [4], Ralf Loewner [4] and Appollonia Aimiosino Okhimamhe [1,5]

1 Climate Change and Human Habitat Programme, West African Science Service Centre on Climate Change and Adapted Land Use (WASCAL CC & HH), Federal University of Technology, Minna 920101, Nigeria
2 Department of Urban and Regional Planning, Federal University of Technology, Minna 920101, Nigeria
3 Department of Soil Sciences and Remote Sensing, Dan Dicko Dankoulodo University of Maradi, Maradi BP 465, Niger
4 Department of Landscape Architecture, University of Applied Science, 17033 Neubrandenburg, Germany
5 Department of Geography, Federal University of Technology, Minna 920101, Nigeria
* Correspondence: kadidjadoulaye@st.futminna.edu.ng

Abstract: Unplanned urban expansion poses significant challenges to environmental sustainability and urban planning. This study analyzes the spatiotemporal dynamics of Zinder's urban landscape using Landsat satellite imagery from 1988, 2000, 2011, and 2022. The study applied remote sensing (RS), geographic information system (GIS) techniques, and urban growth models. The random forest classifier, a machine learning algorithm, was used to classify three land use/land cover categories: "vegetation", "built-up", and "others". Zinder's arid environment is characterized by sparse vegetation, which constitutes a limited but vital component of its landscape. Despite the already sparse vegetation in the area, the findings reveal a 3.5% reduction in vegetation cover between 1988 and 2022, alongside an 11.5% increase in "built-up" areas and an 8% decrease in the "others" category. This loss of already minimal vegetation raises significant concerns about environmental degradation and the exacerbation of desertification risks. Interestingly, urban expansion showed no significant correlation with population growth ($r = 0.29$, $p > 0.5$), suggesting that other factors, such as economic activities, infrastructure development, and land use policies, drive land conversion. Edge expansion emerged as the dominant growth type, with a significant directional preference (Chi-Square = 2334.41, $p < 0.001$) toward major roads and areas with higher accessibility to public services. These findings emphasize the need for strategic urban planning and land management policies to address the drivers of unplanned expansion. Prioritizing sustainable infrastructure development, enforcing land use regulations, and conserving natural landscapes are critical to balancing urban growth with environmental preservation, ensuring resilience and sustainability in Zinder.

Keywords: landscape change; urban sprawl; urban expansion models; optical remote sensing; GIS; Zinder

check for updates

Citation: Doulay Seydou, K.; Morenikeji, W.; Diouf, A.; Dicko, K.; Erdanaev, E.; Loewner, R.; Okhimamhe, A.A. Dynamics of Zinder's Urban Landscape: Implications for Sustainable Land Use Management and Environmental Conservation. *Sustainability* **2024**, *16*, 10263. https://doi.org/10.3390/su162310263

Academic Editor: Hone-Jay Chu

Received: 9 October 2024
Revised: 16 November 2024
Accepted: 18 November 2024
Published: 23 November 2024

Copyright: © 2024 by the authors. Licensee MDPI, Basel, Switzerland. This article is an open access article distributed under the terms and conditions of the Creative Commons Attribution (CC BY) license (https://creativecommons.org/licenses/by/4.0/).

1. Introduction

Analyzing landscape change is essential for assessing environmental sustainability, ecological quality, and impacts of uncontrolled urban expansion over time and across different spatial scales [1,2]. It provides insights into historical and current environmental change patterns, which are crucial for sustainable land management. Over the past few decades, the potential of remote sensing (RS) and geographical information system (GIS) techniques with geostatistical methods has been widely recognized for conducting landscape change analysis [3–5]. The availability of satellite image data covering large areas over extended periods, along with the cost-effectiveness of certain products, enables effective assessment of changes at various spatiotemporal scales [6–8].

Globally, human activities have extensively transformed landscapes, and these changes are expected to continue [9,10]. Urbanization is one of the most significant driving forces behind these alterations [11] as cities increasingly become global economic hubs. This dominance is fueled by the concentration of economic and administrative activities alongside advantages such as enhanced access to healthcare, education, and other essential services. Consequently, urban areas attract populations seeking better opportunities, further accelerating landscape changes and intensifying the impacts of urbanization. In 2018, 55% of the world's population lived in urban areas, and projections indicate that by 2050, this proportion will increase to 68%, with Africa and Asia accounting for approximately 90% of this increase [10]. Migration from rural to urban areas is the primary driver behind this substantial increase in urban population in African nations [12–14], accounting for 40% to 60% of annual urban population growth [15], with some instances reaching as high as 75% [12].

As urban populations rapidly increase, cities expand to accommodate people and their socio-economic activities. While urbanization is fueled by population growth, it has been recognized that urban areas are expanding more rapidly than the urban population in certain regions [16,17]. This rapid urbanization alters land use and land cover (LULC) as well as ecosystem services, presenting a global environmental challenge [18,19]. Additionally, global climate change, characterized by long-term increases in average temperatures and alterations in weather patterns, also impacts the human environment [20,21]. Urban expansion is a primary cause of losses in green spaces and agricultural land and substantially influences climatic variations and human life [22,23]. It is anticipated that this trend will persist due to the projected growth of the world's urban population and the expansion of urban areas. In developing countries such as Niger Republic, urban centers are projected to increase by 5.33% from 2020 to 2025 [10]. Although this might appear slower than in other regions globally, it poses significant challenges due to the country's limited capacity to manage risks and provide adequate safety nets.

In recent decades, monitoring the urban landscape has gained special attention from researchers worldwide [1,24–26], and various quantitative tools have been used to assess urban landscapes. Landscape indices play a significant role in assessing urban growth dynamics, landscape fragmentation, and structural patterns, offering insights into how disturbance impacts ecological balance and environmental sustainability [27]. For instance, indices such as the Shannon Entropy Index (SEI) [28–30] and the built-up area density (BAD) are widely used to assess urban growth and sprawl but have notable limitations regarding detailed spatial analysis. SEI measures the dispersion of urban growth, with higher values indicating more sprawl and lower values reflecting compact growth. However, it only provides an overall measure of sprawl, lacking the ability to differentiate specific growth types [31]. Conversely, BAD quantifies the proportion of developed or constructed areas relative to a specified geographic unit but fails to indicate changes in urban growth patterns over time. The Landscape Expansion Index developed by Lui et al. [27] filled these gaps because it provides a deeper understanding of landscape patterns by capturing both spatial and temporal dynamics. Unlike conventional indices, LEI identifies types of landscape expansion and tracks changes in landscape patterns multiple times. This capability makes LEI especially valuable for analyzing how urban landscapes evolve, offering insights into the sequential processes of urban growth [27].

Despite the increasing attention to urbanization patterns globally [30,32–34], medium-sized cities in developing regions, particularly within the Sahel, remain underrepresented in scholarly research. Zinder, a medium-sized city in Niger, exemplifies this gap. There is a lack of comprehensive analysis of how urban expansion manifests in such settings. Additionally, the interplay between socio-political factors, such as regional instability leading to rural-to-urban migration and urban expansion, has not been investigated in these cities. Understanding the dynamics of medium cities is particularly important as they have greater flexibility to adapt their development pathways, unlike megacities, which have often established entrenched growth patterns that are challenging to reverse. This study

seeks to fill these gaps by providing a detailed examination of Zinder's urban expansion, utilizing advanced spatial analysis such as the Landscape Expansion Index (LEI) and Urban Expansion Index (UEI), which are yet to be applied to this context, to inform sustainable urban planning efforts. Zinder is ranked as the second-fastest growing city in Africa between 2020 and 2035, with a projected growth rate of 118% [35]. This remarkable growth makes Zinder a critical example of rapid urbanization in sub-Saharan Africa, where cities face unique challenges in sustainable development and resource management. Increased insecurity in Niger and neighboring countries, such as Nigeria and Chad, has driven rural communities to seek safety in cities, including Zinder. The city has become a refuge for people fleeing Boko Haram attacks from Nigeria and nearby villages [36].

This study comprehensively examines land use/land cover (LULC) changes, urban growth dynamics, and expansion patterns in Zinder from 1988 to 2022. The objectives are threefold: (i) to quantify LULC trends and analyze their relationship with population growth; (ii) to assess different urban growth types and identify key drivers behind these growth patterns; and (iii) to evaluate the spatial preferences in urban expansion. This study hypothesizes that (i) population growth significantly drives LULC changes and that (ii) directional preferences in expansion correlate with proximity to major roads and economic zones.

2. Materials and Methods

2.1. Study Area

This study was conducted in Zinder, a Sahelian city in Niger Republic. Zinder is a significant location for this study due to its urban growth patterns and the environmental challenges it faces. Locally known as Damagaram, it is the second-largest city in Niger, following the capital city, Niamey. It is located within latitude 13°44′ N, and 13°54′ N and longitude 8°54′ E and 9°40′ E (Figure 1), and it was Niger's first capital city. The city is experiencing a population increase from just 12,466 in 1950 to 600,961 in 2024 [37]. Indeed, since 2002, Zinder has experienced a higher population growth rate than Niamey (5.15% compared to 4.11% in 2024). As the capital of the region, Zinder has recently faced extreme migration, mainly due to Boko Haram conflicts, which have driven people to seek safety and well-being in neighboring cities [36]. Zinder is being transformed into a modern city in terms of infrastructure development and industry. Therefore, it is necessary to plan for urban expansion.

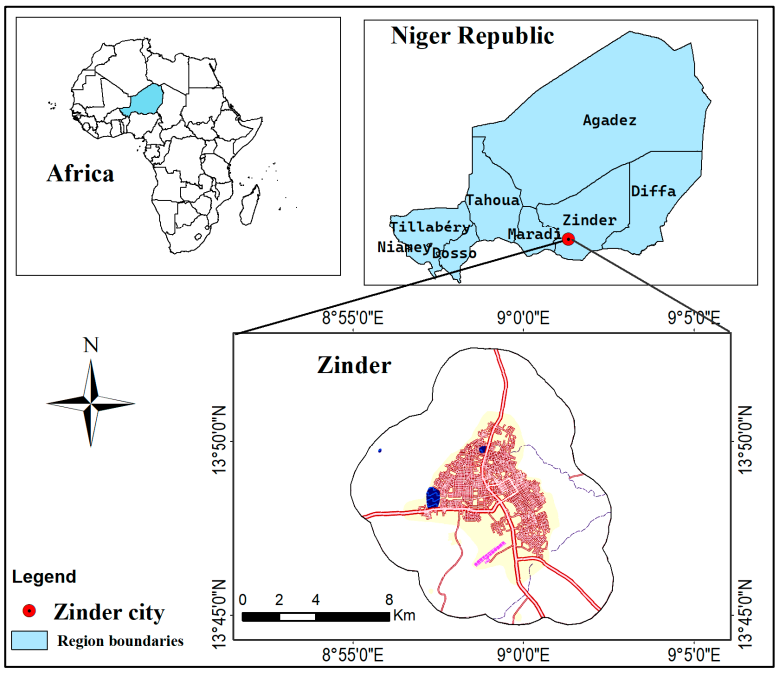

Figure 1. Location of the study area with road network.

2.2. Datasets

This study used multispectral Landsat satellite images to analyze land use/land cover (LULC) changes. Landsat was selected for its extensive history of continuous, high-resolution observations, which makes it an invaluable resource for monitoring long-term urban expansion trends and supporting land management decisions [5,23,38]. Specifically, images from 1988, 2000, 2011, and 2022 were chosen based on seasonal availability, image quality, and coverage, with each scene representing a study period to capture key urban growth patterns effectively. All images were accessed through the USGS Earth Explorer platform (https://earthexplorer.usgs.gov/) (Table 1).

Table 1. Satellite images were used in the study.

Satellite	Sensor ID	Path/Row	Spatial Resolution	Cloud Cover (%)	Acquisition Date
Landsat 8	OLI_TIRS	188/51	30 m	0.02	10 April 2022
Landsat 7	ETM	188/51	30 m	0.00	20 April 2011
Landsat 7	ETM	188/51	30 m	5.00	05 April 2000
Landsat 4	TM	188/51	30 m	0.00	19 March 1988

2.3. Image Processing and Classification

The Landsat images used in this study were radiometrically calibrated and orthorectified by the data provider to correct sensor-related errors and align the imagery with true geographic coordinates. Further rectification and enhancement steps were conducted to ensure the data's reliability for land use/land cover (LULC) classification. These preprocessing steps included atmospheric correction using Dark Object Subtraction (DOS), pan-sharpening, reprojection, clipping, and color composite creation. Each step had a specific impact on data quality and interpretability [39–41].

Atmospheric correction via DOS was applied to reduce atmospheric scattering and absorption effects, minimizing brightness distortions and improving the clarity of surface reflectance. This correction ensures that the reflectance values more accurately represent the land surface, enhancing differentiation between LULC types. The pan-sharpening process improved spatial resolution from 30 m to 15 m by merging the multispectral bands with the panchromatic band, making it possible to detect finer details. This step is particularly useful in identifying small urban features, which are essential for accurate LULC classification [39].

The images were reprojected to WGS 1984 UTM Zone 32N to align with the study area's geographic region, ensuring accuracy in spatial measurements and consistency across datasets from different years. Clipping the images to the area of interest (AOI) reduced data volume and focused the analysis on relevant locations, minimizing extraneous data that could affect classification accuracy. Finally, a color composite was created by combining multiple spectral bands to improve visual interpretation, which assists in distinguishing different LULC classes by enhancing color contrast.

These preprocessing steps collectively contribute to image quality, correct distortions, and enhance visual interpretability, ultimately improving the accuracy of the subsequent [41]. After preprocessing, representative sample data for each LULC class were generated based on visual interpretation, ground truth data, and ancillary sources, including Google Earth imagery, OpenStreetMap, and topographical maps. The Dzetsaka Classification Plugin in QGIS was used to perform a supervised classification. This plugin supports multiple algorithms, including the Gaussian Mixture Model, random forest, and Support Vector Machine (SVM), enabling users to perform efficient and accurate classifications within the QGIS environment using various classification techniques. These algorithms were tested, and the RF [42] provided the highest accuracy. Therefore, it was used to perform a supervised classification of the images. The RF algorithm excels at LULC classification and remote sensing because it can handle complex datasets, is robust against overfitting, and has low bias [43,44]. During the training phase, it creates an ensemble of decision trees that are trained independently; the results from all trees are then aggregated

to provide a prediction [45–47]. During the classification, 80% of the sample data were used to train the algorithm, while the remaining 20% was reserved for accuracy assessment. The classification accuracy was evaluated by computing user accuracy, producer accuracy, overall accuracy, and Kappa coefficient indices. Equations (1) and (2) calculate overall accuracy and the Kappa coefficient. All the above operations were performed in QGIS 3.34 software, chosen for its open-source accessibility, extensive geospatial analysis tools, and compatibility with diverse data formats.

$$\text{Overall accuracy} = \frac{\sum_{i=1}^{r} x_{ii}}{N^2} \quad (1)$$

$$\text{Kappa coefficient } (\hat{K}) = \frac{N(\sum_{i=1}^{r} x_{ii}) - \sum_{i=1}^{r}(x_{i+}x_{+i})}{N^2 - \sum_{i=1}^{r}(x_{i+}x_{+i})} \quad (2)$$

$(\hat{K})$ = Kappa coefficient.
r is the number of rows in the matrix.
x_{ii} is the number of observations in row i and column i.
x_{i+} and x_{+i} are marginal totals for row i and column i, respectively.
N is the total number of observations.

The LULC classes were reclassified into built-up and non-built-up categories for further analysis. The workflow of the study, including the classification and reclassification steps, is illustrated in Figure 2.

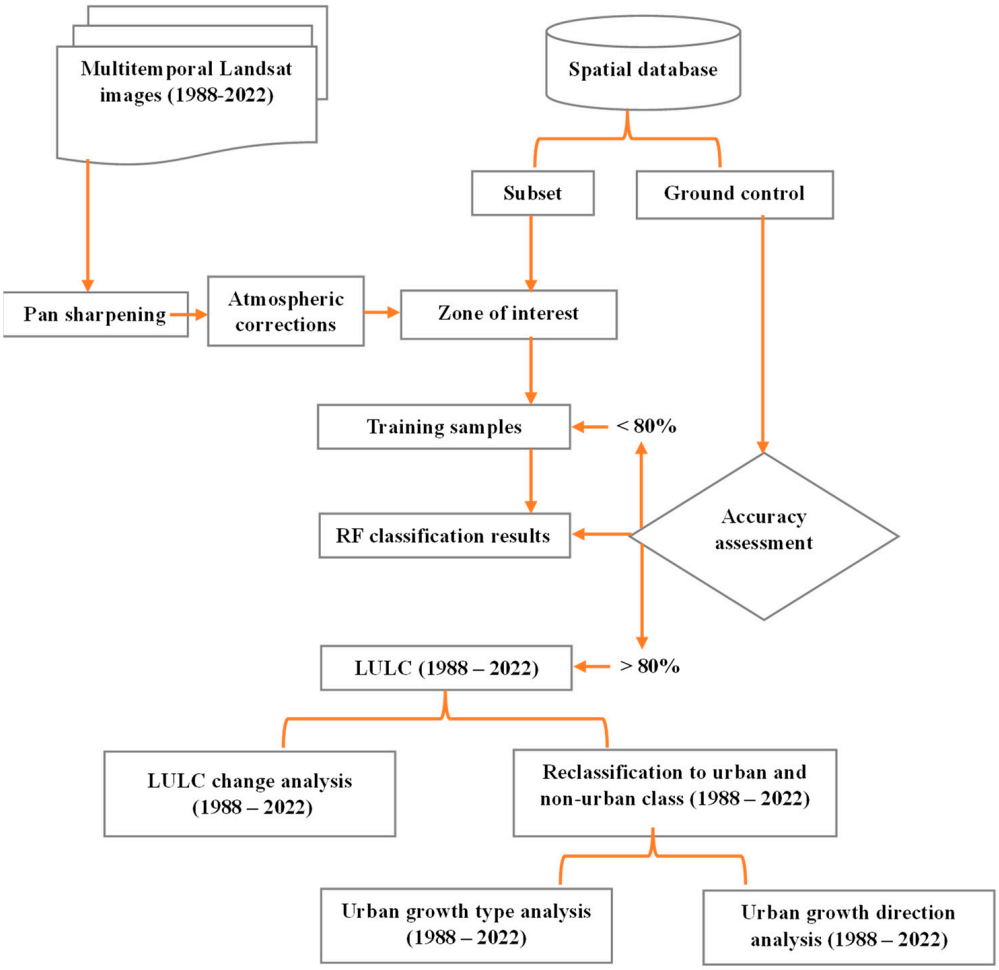

Figure 2. Methodological flowchart adopted for the study.

2.4. Analysis of Land Use and Land Cover Change

The study period of 34 years from 1988 to 2022 was segmented into three distinct intervals called hereby intermediates periods: T1 (1988–2000), T2 (2000–2011), and T3 (2011–2022). This segmentation was implemented to enhance the analysis of LULC changes using the SCP plugin within the QGIS software environment. The methodology involved a comparative assessment of LULC across successive periods (e.g., 1988 and 2000) to quantify spatiotemporal changes. For each defined LULC category, area calculations were performed at each specified time point. Subsequently, a transition matrix was generated to elucidate the dynamics between various classes over time and space. To further investigate the relationship between population growth and urban development, a simple linear regression analysis was conducted to determine if population size significantly predicted the expansion of the built-up area from 1988 to 2022.

2.5. Urban Growth Patterns

Urban growth direction analysis used built-up areas extracted from LULC maps. The analysis employed sixteen gradient directions: "North (N), North North-East (NNE), North-East (NE), East North-East (ENE), East (E), East South-East (ESE), South-East (SE), South South-East (SSE), South (S), South South-West (SSW), South-West (SW), West South-West (WSW), West (W), West North-West (WNW), North-West (NW), and North North-West (NNW)". The central business district (CBD), identified around the Grand Marché during a field visit, served as the reference point for the directional analysis. A Chi-Square Goodness of Fit test was performed to assess whether urban growth in Zinder exhibits a directional preference. This test compared the observed urban expansion across various directions against the expected uniform distribution of growth. Furthermore, the study area was segmented into five concentric zones using 2 km equidistant buffer rings from the city center to assess whether urban growth exhibited a dispersed or compact pattern [48]. For each buffer zone, the Urban Density Index (UD) was computed using Equation (3) to assess the density of urban expansion. Similarly, the Urban Expansion Intensity Index (UEII) was computed for these zones using Equation (4) to identify urban growth preferences during specific periods [27,49,50].

$$D_i = \frac{a_i}{A_i} \tag{3}$$

D_i = the density of the ring i.
a_i = the built-up area of the ring i.
A_i = The area of the ring i.

$$UEII_i = \frac{ULA_i^{t_2} - ULA_i^{t_1}}{TLA_{\,i} \times \Delta t} \times 100 \tag{4}$$

where $UEII_i$ is the Urban Expansion Intensity Index of the zone i; $ULA_i^{t_2}$ and $ULA_i^{t_1}$ are the built-up area at the time t_2 and t_1 respectively; TLA_i is the total area of the zone i and Δt is the study period between the two dates. The standard division of UEII values is UEII > 1.92 is "high-speed"; 1.05 ≤ UEII ≥ 1.92 is "fast"; 0.59 ≤ UEII ≥ 1.05 is "medium speed"; values 0.28 ≤ UEII ≥ 0.59 is "low-speed"; and 0 ≤ UEII ≥ 0.28 is considered "slow" [31,51].

2.6. Urban Growth Types

In this study, the Landscape Expansion Index (LEI) developed by Lui et al. [27] was used to quantify three types of urban growth: infilling, edge expansion, and outlying (Figure 3). Initially, the urban landscape was categorized as "old" (present in both initial and subsequent periods) and "new" (emerging in the later period). Using an urban change map, LEI values were calculated through buffer analysis, comparing the mutual edge length and perimeter of objects (Equation (5)) using the LEI tool in ArcGIS Pro [27,52]. The selection of the 200 m buffer zone was determined after a sensitivity analysis using different buffer zone values, including 1 m and 50 m used by previous studies in other parts

of the world [27]. Each buffer result was compared against Google Earth imagery, which revealed that smaller values overestimated outlying growth types. In comparison, larger values underestimated the outlying type due to the specific housing morphology of the study area. Consequently, the 200 m buffer aligned most accurately with LEI calculations and spatial dynamics. The range of LEI values is 0 to 100. The values were then classified into urban growth types following the standardized values division as follows: infilling ($100 \geq LEI > 50$), edge expansion ($50 \geq LEI > 0$), and outlying ($LEI = 0$) [27].

$$LEI = \frac{l_c}{P} \times 100 \quad (5)$$

l_c = length of the shared edge.
P = perimeter of the new object.

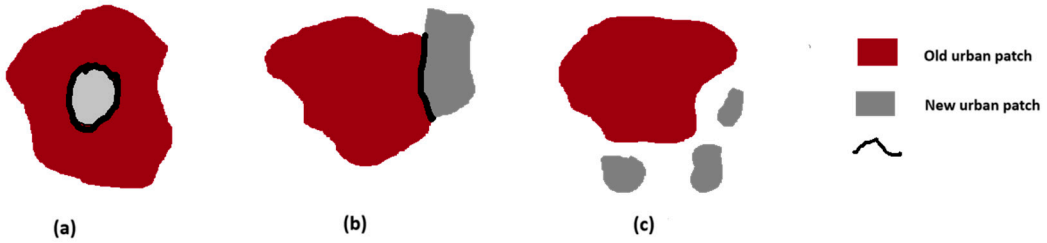

Figure 3. Types of landscape expansion: (**a**) infilling; (**b**) edge expansion; (**c**) outlying.

3. Results

3.1. Assessment of LULC Change

Three LULC classes were identified in the study area: built-up areas, vegetation, and others (Figure 4). The descriptions of these classes are provided in Table 2. The Kappa coefficient values were 88.6%, 92.1%, 91.2%, and 95.3% for the years 1988, 2000, 2011, and 2022, respectively. Correspondingly, the overall accuracy values were 97.1%, 98.2%, 98.3%, and 98.6% for the same years. The reduced accuracy for 1988 is primarily due to the limitations in the quality and spectral sensitivity of the Landsat 4 sensor, which is lower than that of the Landsat 7 and Landsat 8 sensors used in 2000, 2011, and 2022. Landsat 4's Thematic Mapper (TM) sensor has broader spectral bands and lower radiometric resolution [53], making it more challenging to distinguish between certain land cover types. Despite these limitations, the data provides valuable historical insights, and rigorous processing was applied to achieve the highest possible accuracy (88.6%). The accuracy metrics obtained indicate that the classification results are highly reliable (Congalton, 1991).

Table 2. Description of LULC classes.

Class Name	Class Description
Vegetation	Moderate vegetation cover, including shrubs, plantation, and tree gardens.
Built-up	Residential areas, including urban, industrial, commercial, and all kinds of roads.
Others	Bare land, rocks, and agricultural lands.

The analysis of LULC changes revealed that the three land use categories exhibited varying rates of change over time (Figure 5a). Throughout the study period, the "others" class consistently dominated the landscape, covering more than 80% of the total area. During the first period (T1), this class increased by 1.67%, primarily due to a reduction in the vegetation class. However, in the subsequent periods (T2), the "others" class decreased by 7.01% and 2.64%, respectively (Figure 5b). This decline coincided with a significant expansion of built-up areas, which increased by 11.5% from 1988 to 2022.

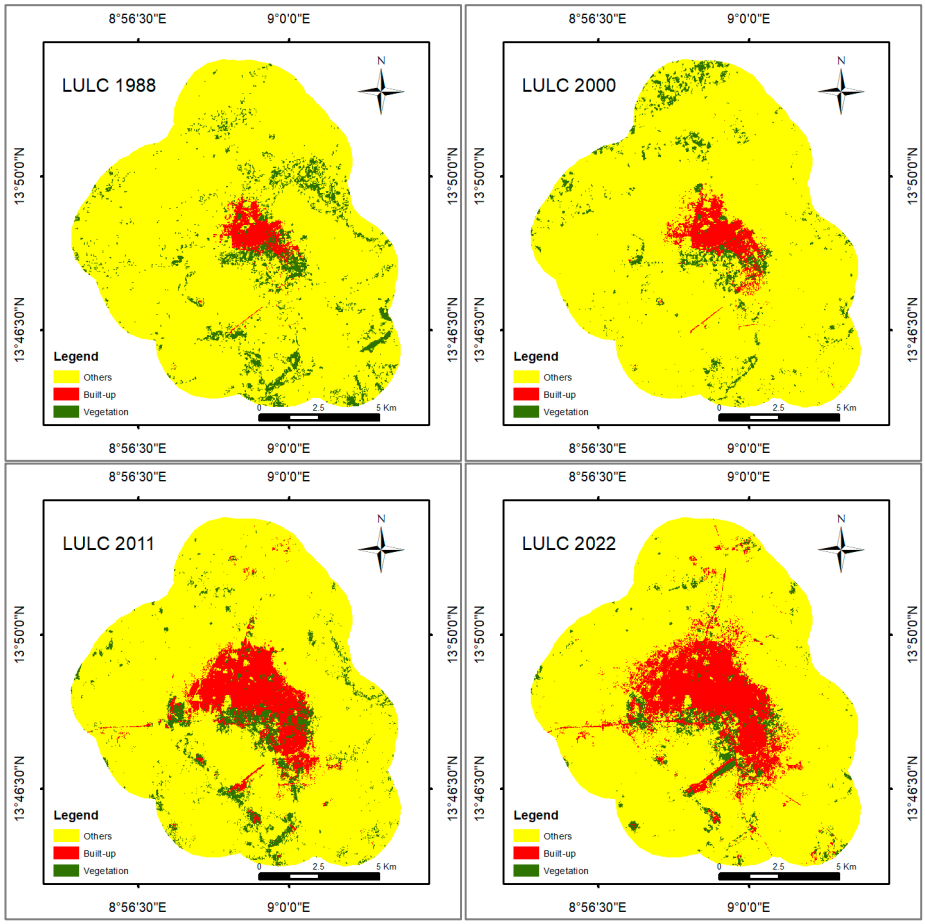

Figure 4. Classified LULC of Zinder from 1988 to 2022.



Figure 5. (**a**) Proportion of LULC from 1988 to 2022. (**b**) Proportion of LULC area change.

The transition matrix (Table 3) offers detailed insights into the conversions between different LULC classes throughout the study period, highlighting the specific changes from one class to another.

Table 3. Transition matrix.

1988	**2000**	**Vegetation**	**Built-up**	**Others**	**Total**
	Vegetation	1.63	0.46	5.64	7.73
	Built-up	0.00	2.51	0.00	2.51
	Others	3.13	0.84	85.80	89.76
	Total	4.76	3.80	91.44	100
2000	2011	Vegetation	Built-up	Others	Total
	Vegetation	1.73	0.43	2.61	4.77
	Built-up	0.00	3.80	0.00	3.80
	Others	4.57	5.05	81.81	91.43
	Total	6.30	9.28	84.42	100
2011	2022	Vegetation	Built-up	Others	Total
	Vegetation	2.13	0.90	3.27	6.30
	Built-up	0.00	9.28	0.00	9.28
	Others	2.05	3.86	78.51	84.42
	Total	4.18	14.04	81.78	100

The analysis of built-up area growth rates for the three intermediate periods (Table 4) reveals a differential growth rate. The most significant increase in the built-up area, at 144.15%, occurred during the second intermediate period.

Table 4. Buit-up area and population growth rate (%).

Intermediate Period	**T1**	**T2**	**T3**
Built-up area growth rate (%)	51.66	141.15	33.90
Population growth rate [1] (%)	39.16	78.44	82.21

[1] Source: Zinder Population [37].

When comparing the growth rates of the built-up area and population, it was expected that the built-up area growth rate during the last intermediate period (T3) would be more substantial, given the highest population growth rate observed during the same period [37]. However, the results did not verify this expectation. The regression analysis further indicated a weak (r = 0.29) and non-statistically significant correlation (p = 0.83), suggesting that population growth alone did not significantly predict the growth rate of the built-up area. This suggests that other factors may be influencing urban expansion in Zinder.

3.2. Analysis of Urban Growth Types

The analysis identified three types of urban growth in Zinder: infill, edge expansion, and outlying growth (Figure 6). The predominant growth type was edge expansion, which accounted for over 90% of the total urban growth from 1988 to 2022. Outlying growth was the second most common type, while infill growth contributed the least, representing less than 1% of the total growth (Figure 7).

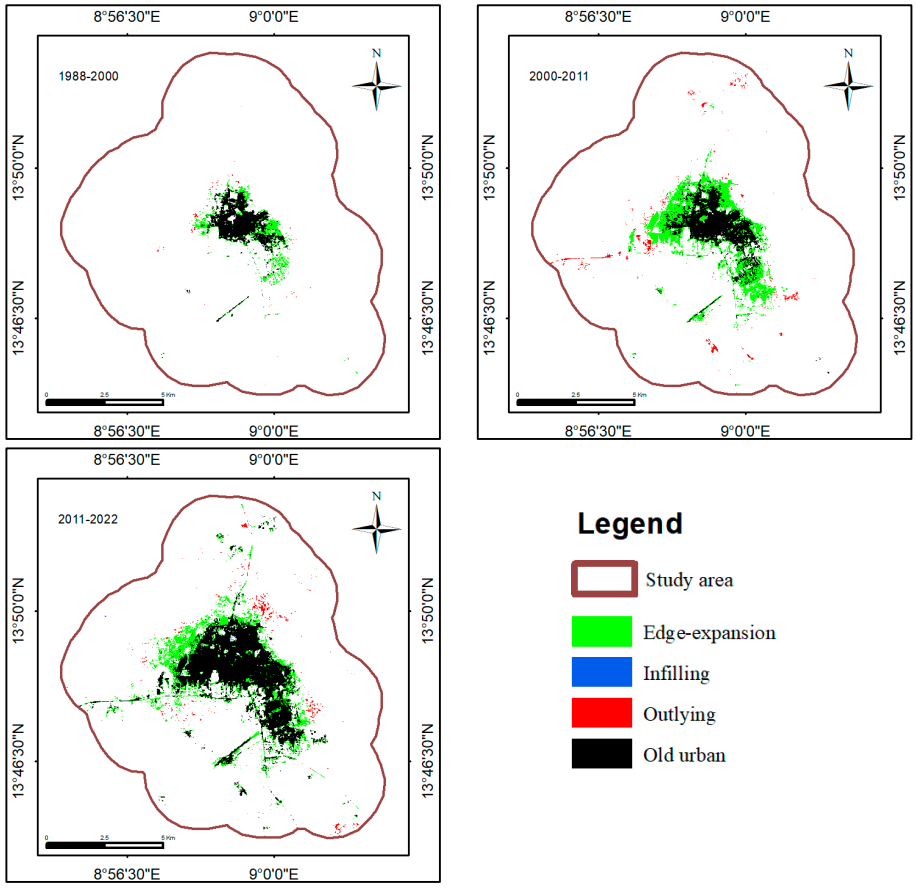

Figure 6. Urban growth types from 1988 to 2022.

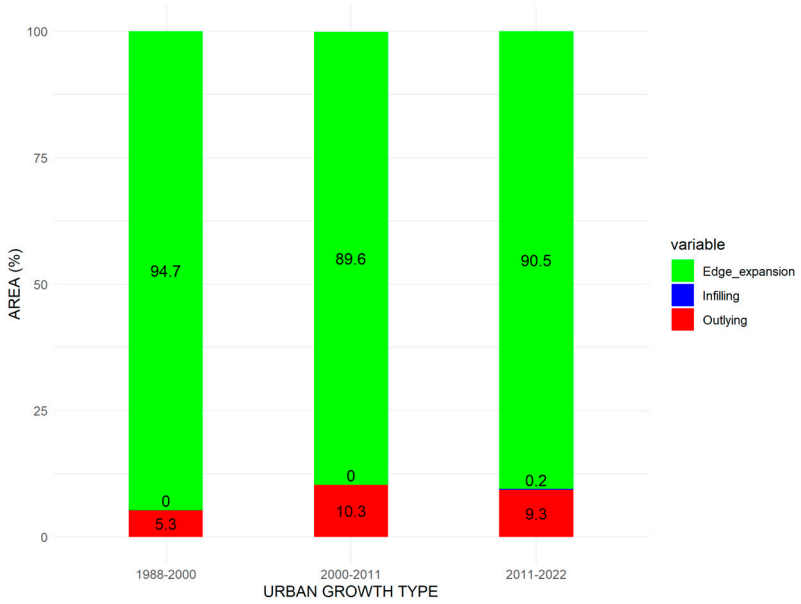

Figure 7. Proportion of urban growth type per intermittent period.

3.3. Analysis of Urban Growth Direction and Pattern

The direction of urban growth in Zinder has varied over the past 34 years, influenced by both spatial and temporal factors. The results of the Chi-Square goodness-of-fit analysis (Chi-Square Statistic: 2334.41 and *p*-value: 0.0) indicate a statistically significant directional preference in urban growth ($p < 0.05$). This allows us to reject the null hypothesis of uniform

distribution. This confirms that urban expansion in Zinder is not evenly distributed. Instead, it demonstrates significant growth in specific directions, particularly NNW-WSW and SE-SSE, as highlighted in Figure 8. The observed directional growth aligns with major roads and key landmarks, likely influencing these patterns. In the NNW direction, we find the National Road 11 (RN11), which runs 8.5 km through Zinder toward Agadez. This road leads to significant landmarks, including André Salifou University, a military camp, the Zinder refinery (SORAZ), and educational institutions such as Saint Joseph and Dan Bassa. In the SE and W directions, the expansion is aligned with National Road 1 (RN1), the main artery connecting Zinder to Niamey, the capital city of Niger.

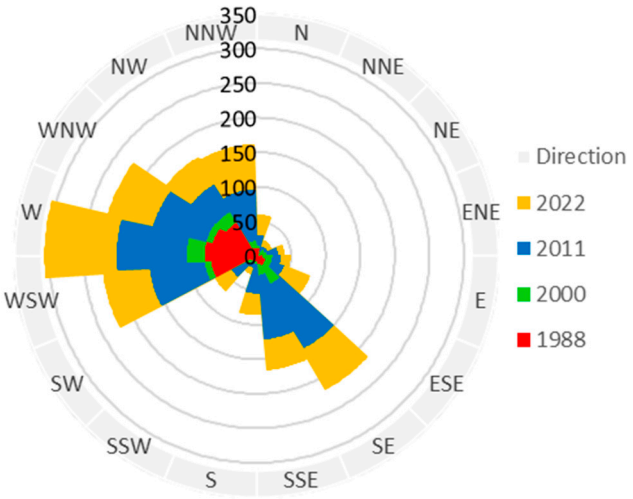

Figure 8. Urban growth direction from 1988 to 2022 in hectares.

The city of Zinder is experiencing compact growth, as evidenced by the increasing density of built-up areas within each buffer zone from 1988 to 2022, with higher values observed from the city center to the periphery (Figure 9). This trend highlights a preference for expansion within the first buffer zone.

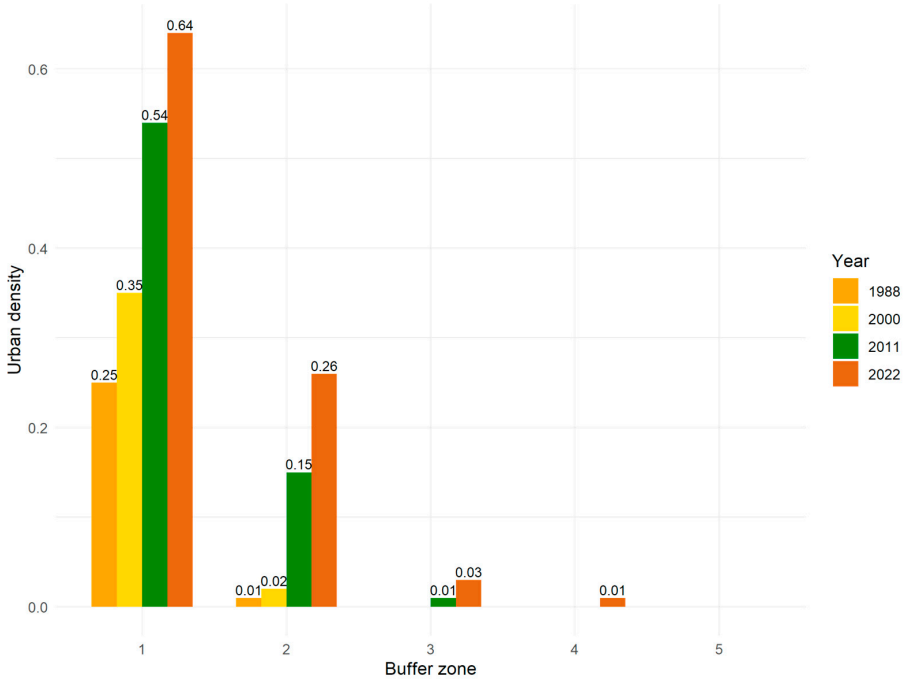

Figure 9. UD by buffer zone from 1988 to 2022.

Further insights into expansion preferences were provided by the Urban Expansion Intensity Index (UEII) values. During the first and second intermediate periods, buffer zone 1 was the primary area for expansion, with UEII values of 0.78 and 0.9 in the first and third periods, indicating medium growth speed, while the second period showed rapid growth. By the last intermediate period, the available land in the first inner ring had decreased to saturation, resulting in medium growth speeds shifting to ring 2. Meanwhile, the remaining zones exhibited slow growth throughout the study period, with growth rates progressively decreasing from the center to the periphery (Table 5). These findings reinforce a compact growth pattern in Zinder, characterized by densification near the city center and gradual outward expansion.

Table 5. UEII by buffer zone per intermediate period.

Ring ID	T1	T2	T3
1	0.78	1.76	0.91
2	0.01	0.05	1.00
3	0.00	0.00	0.17
4	0.01	0.01	0.08
5	0.00	0.00	0.01

4. Discussion

4.1. The Dynamics of LULC

Over the past 34 years, Zinder has undergone significant changes in LULC, characterized by a notable decrease in vegetation and natural land covers, alongside an increase in built-up areas (Figure 5). This same pattern was observed by other studies across the world, including Qoam City [54], Abha City [55], Mangarulu [31], and Niamey, the capital city of Niger [17,56]. In the Zinder region, over 80% of the population is engaged in agriculture; this expansion of built-up areas has led to the conversion of agricultural land, impacting food security and reducing agricultural productivity due to a decline in the number of farms and soil degradation [57]. Urban expansion and population growth have also exerted anthropogenic pressure on natural resources, reducing vegetation cover through deforestation for energy and construction materials [58].

Interestingly, there was a 1.53% increase in vegetation cover during the second intermediate period, possibly due to government programs promoting assisted natural regeneration and irrigation schemes to combat desertification [59]. These regeneration activities are effective ways to conserve vegetation cover in arid and semi-arid regions, and their effectiveness has been heightened in Chadakori and Saé Saboua [60]. On the other hand, the SORAZ oil refinery development may have intensified urban expansion activities, leading to the highest growth rate of built-up areas at 144.15% during the second intermediate period (Table 4). The third period witnessed the most significant population growth, driven by rural-to-urban migration due to Boko Haram attacks; however, this did not correspond with a proportional increase in built-up areas, as many displaced individuals lacked the financial means for permanent housing [36]. This economic barrier explains the weak and statistically insignificant regression results between built-up area growth and population dynamics in Zinder, indicating that urban expansion, in this case, was more closely linked to infrastructural and economic developments than to direct population growth. This result is contrary to the findings of Das et al. [61] in the Barrackpore Subdivision area, India, and of Huang et al. [62] in nine urban agglomerations in China.

To promote coherent development, Zinder has established a reference document for any development within the district, created independently at the district level rather than citywide. Districts have the authority to convert farmlands into plots and sell them, generating income for the district. However, this has led to unregulated land conversion and plot sales, further reducing agricultural areas. In all four documents from the urban districts that make up the city, urban expansion strategies were not addressed. Additionally, all of

these documents are outdated and have not been updated, indicating a lack of planning for urban expansion. Consequently, the city continues to grow in a disorganized manner.

4.2. Urban Growth Types and Patterns

In the reviewed literature, the terms "urban growth" and "sprawl" are often used interchangeably to analyze changes in urban landscapes [30,32–34]. However, it is essential to recognize that not all urban growth can be considered as urban sprawl. Critics argue that urban sprawl results in inefficient and costly development while contributing to air pollution due to increased fuel consumption in transportation. Consequently, labeling all forms of growth as sprawl creates a negative perception of development. Certain types of growth, such as infill development, are beneficial as they conserve resources, contrasting with the negative connotations associated with urban sprawl [63–65]. To accurately classify a specific type of growth as urban sprawl, it is essential to quantify urban growth based on the areas affected and the nature of the changes. This approach allows for a more nuanced understanding aligned with the study's objectives rather than categorizing all growth as sprawl [66,67]. In Zinder, edge expansion and outlying growth types are the dominant patterns (Figure 7), indicating that the city is experiencing sprawl. Infill growth, which is the least growth type, involves newly developed patches, filling gaps between or within older patches. This method makes efficient use of available land within developed areas [68] and promotes effective land resource management [69]. Conversely, edge expansion refers to a pattern of progressive outward migration from the periphery of urban areas; this type of development is often referred to as metropolitan or urban fringe development [70]. Outlying growth occurs when a new patch has no neighboring relationship with an existing one, which Heimlich and Anderson [70] describe as development outside the urban fringe. In all cases, the existing built-up area plays a crucial role in determining the type of urban growth.

Zinder's housing landscape is characterized by three main types: clay housing, a combination of clay and concrete housing, and concrete housing. In the 3rd district of Zinder, clay and concrete housing predominates, making up 47.1% of the total building in the district compared to only 20.90% for concrete housing [71]. This trend is consistent throughout the study area. The low percentage of concrete housing can be attributed to the financial conditions of the population. Historically, Zinder faced significant water issues until 2008. Consequently, the high cost of accessing water led homeowners to opt for clay and cement to reduce construction expenses [71]. This situation resulted in one-story buildings being more common than multi-story structures. However, newly developed areas are increasingly featuring multi-story buildings and concrete housing. This historical context may explain the prevalence of edge-expansion growth observed in this study.

It is important to note that the city center is the most densely populated area, with a preference for expansion extending 2 km around the Central Business District (CBD) until land saturation occurs (Figure 7). Developing new built-up areas heavily relies on road networks and proximity to public services. Roads play a pivotal role in socioeconomic development by facilitating access to essential services, enhancing trade opportunities, and improving overall quality of life. A similar result was observed in Qom City based on population density mapping [54] and in Purulia Municipality, based on Shannon entropy values and gradient direction analysis [5].

4.3. Policy Implications

This study highlighted the rapid urban expansion and a trend toward urban sprawl in Zinder. However, urban sprawl is not an ideal development pattern, as it leads to inefficient use of land resources [64]. It also causes environmental challenges, such as increased air pollution from transportation, landscape fragmentation, and transport inefficiency [63], as well as disparities in public services across the city. To mitigate these effects, sustainable urban planning strategies are required. Municipalities should plan for urban growth and implement policies that maximize the use of available space while encouraging the

development of multiple housing units within a single compound rather than the single housing compounds currently prevalent in the city. Additionally, effective road networks are necessary to facilitate urban development. Enhancing these networks is crucial for influencing how urban land is used and for directing changes in the urban environment [72]. The effectiveness of the urban plan depends on the inclusion of all social groups and the consideration of all socio-economic sectors. Furthermore, adopting energy-efficient stoves and exploring alternative building materials instead of wood can reduce pressure on natural resources. Diversifying the local economy beyond agricultural activities is vital for promoting more balanced and resilient development. Preserving agricultural land and ensuring sustainable agricultural practices are critical for maintaining food security in the area, especially given its vulnerability to urban expansion. Promoting urban forestry is also important for improving living conditions and the environment. This integrated approach is essential for addressing social and environmental challenges faced by urban areas, in general, and Zinder, in particular, thereby making the city resilient, inclusive, and sustainable.

4.4. Limitations and Future Perspectives

Despite the importance of Zinder in Niger Republic and the challenges posed by LULC changes due to urban growth, no similar studies have been published for this area. The lack of comparable research presents a challenge in aligning our findings with existing literature, positioning this study as a pioneering effort. Another limitation pertains to the spatial resolution of the Landsat images used. Although the Landsat images were instrumental in achieving our objectives, their 30 m resolution may have led to a slight underestimation of built-up areas, particularly in Zinder, where many structures are constructed from clay and vegetation. To assess this limitation, we conducted a comparative analysis using Sentinel-2 imagery from the same date in 2022. Sentinel-2 provides a finer 10 m resolution that enhances the detection of smaller and fragmented urban features. However, this comparison was possible only for 2022, as Sentinel-2 data are unavailable for earlier years in our study period (1988, 2000, and 2011). The results revealed a 3.5% difference in built-up area estimates, with Landsat underestimating the extent of built-up areas. This discrepancy highlights the importance of high-resolution data in accurately capturing urban boundaries, especially in mixed or sparsely built landscapes. Future studies could benefit from incorporating high-resolution imagery, such as PlanetScope, SPOT, and RapidEye, to capture even more detailed and accurate representations of urban areas. Additionally, advancements in downscaling techniques could further mitigate underestimation issues, providing more reliable data for urban studies in regions with similar land-cover characteristics. Moreover, recent advancements in deep learning offer promising tools for LULC analysis and urban studies. For example, manifold regularization-based deep convolutional autoencoders (MR-DCAEs) have shown significant potential in feature extraction and anomaly detection within high-dimensional data [73]. Originally developed for applications like unauthorized broadcasting identification, MR-DCAE, and similar deep learning architectures like Convolutional Neural Networks (CNNs) [74] could be adapted for LULC classification and detecting subtle urban landscape changes.

Finally, future research could expand on this study by incorporating sustainability indicators into the analysis of LULC changes. This approach would assess the environmental impacts of urban expansion, including effects on local ecosystems and resource demands. Indicators such as water and energy consumption, greenhouse gas emissions, and green space loss could be used to quantify the environmental costs of growth. Social equity metrics could also help evaluate how urban expansion affects different population groups, particularly regarding access to essential services and housing. Integrating these sustainability indicators will provide a more nuanced view of urban growth dynamics and contribute to developing sustainable urban planning strategies for Zinder.

5. Conclusions

This study utilized remote sensing (RS) and geographic information system (GIS) techniques, along with an urban growth model, to comprehensively characterize and quantify urban landscape changes in Zinder City over a 34-year period. Additionally, the relationship between the growth of built-up areas and urban population growth was assessed through simple linear regression analysis based on available population data. The findings revealed that LULC changes were predominantly driven by the conversion of vegetation and agricultural lands into built-up areas. This poses significant implications for food security, as agriculture remains the primary livelihood for over 80% of the population in the study area. Despite the general association between population growth and urban expansion, the study found no significant relationship between these two variables in Zinder. This suggests that other factors, such as land availability and infrastructure development, may play a more pivotal role.

The study's results on how proximity to infrastructure drives urban expansion provide valuable insights for infrastructure planning. By understanding these growth patterns, urban planners can strategically design infrastructure to guide future development to minimize impacts on ecologically sensitive areas. Additionally, the findings highlight significant land use conflicts, particularly the conversion of agricultural and vegetative lands into built-up areas. This trend emphasizes the importance of protecting essential green spaces and agricultural land, which are critical not only for maintaining food security but also for preserving environmental health. Together, these insights offer practical guidance for balancing human development with environmental preservation in Zinder and similar urban areas.

To address these challenges practically, the development of comprehensive City Development Strategies (CDSs) is essential. Such strategies should involve strategic interventions from public, private, and civil society stakeholders to guide the city's growth and improve urban performance.

Supplementary Materials: The following supporting information can be downloaded at: https://www.mdpi.com/article/10.3390/su162310263/s1.

Author Contributions: Conceptualization, methodology, validation, software, formal analysis, investigation, resources, data curation, writing—original draft preparation, visualization, project administration, K.D.S.; funding acquisition, K.D.S. and A.A.O.; supervision, W.M., A.D. and R.L.; writing—review and editing, A.D., W.M., E.E., K.D. and A.A.O. All authors have read and agreed to the published version of the manuscript.

Funding: This research is part of a doctoral research project funded by the German Federal Ministry of Education and Research (BMBF), which provided financial support and implemented by the West African Science Service Centre on Climate Change and Adapted Land Use (WASCAL) and the Federal University of Technology, Minna, Nigeria, which contributed expertise and resources.

Institutional Review Board Statement: Not applicable.

Informed Consent Statement: Not applicable.

Data Availability Statement: The original contributions presented in the study are included in the Supplementary Materials; further inquiries can be directed to the corresponding author.

Acknowledgments: The authors acknowledge the support of the Climate Change and Human Habitat Programme staff, West African Science Service Centre on Climate Change and Adapted Land Use (WASCAL CC & HH), Federal University of Technology Minna, Nigeria. They also acknowledge the use of ChatGPT, an AI language model developed by OpenAI, to help refine the manuscript's language and clarity.

Conflicts of Interest: The authors declare no conflicts of interest.

References

1. Abbas, Z.; Yang, G.; Zhong, Y.; Zhao, Y. Spatiotemporal change analysis and future scenario of lulc using the CA-ANN approach: A case study of the greater bay area, China. *Land* **2021**, *10*, 584. [CrossRef]
2. Olorunfemi, I.E.; Fasinmirin, J.T.; Olufayo, A.A.; Komolafe, A.A. GIS and remote sensing-based analysis of the impacts of land use/land cover change (LULCC) on the environmental sustainability of Ekiti State, southwestern Nigeria. *Environ. Dev. Sustain.* **2020**, *22*, 661–692. [CrossRef]
3. Kumar, K.S.; Kumari, K.P.; Bhaskar, P.U. Application of Markov chain & cellular automata based model for prediction of Urban transitions. In Proceedings of the International Conference on Electrical, Electronics, and Optimization Techniques, ICEEOT, Chennai, India, 3–5 March 2016; Institute of Electrical and Electronics Engineers: Piscataway, NJ, USA, 2016; pp. 4007–4012.
4. Adhikari, S.; Southworth, J. Simulating forest cover changes of Bannerghatta National Park based on a CA-Markov model: A remote sensing approach. *Remote Sens.* **2012**, *4*, 3215–3243. [CrossRef]
5. Shikary, C.; Rudra, S. Measuring Urban Land Use Change and Sprawl Using Geospatial Techniques: A Study on Purulia Municipality, West Bengal, India. *J. Indian Soc. Remote Sens.* **2020**, *49*, 433–448. [CrossRef]
6. Attri, P.; Chaudhry, S.; Sharma, S. Remote sensing & GIS based approaches for LULC change detection—A review. *Int. J. Curr. Eng. Technol.* **2015**, *5*, 12.
7. Cheruto, M.; Kauti, M.; Kisangau, D.; Kariuki, P. Assessment of land use and land cover change using GIS and remote sensing techniques: A case study of Makueni County, Kenya. *J. Remote Sens. GIS* **2016**, *5*, 4. [CrossRef]
8. Barros, J.X. *Urban Growth in Latin American Cities Exploring Urban Dynamics Through Agent-Based Simulation*; University College London: London, UK, 2004.
9. Stephens, C.M.; Lall, U.; Johnson, F.M.; Marshall, L.A. Landscape changes and their hydrologic effects: Interactions and feedbacks across scales. *Earth Sci. Rev.* **2021**, *212*, 103466. [CrossRef]
10. United Nations. *World Urbanization Prospects: The 2018 Revision*; United Nations: New York, NY, USA, 2018; pp. 9–31.
11. Bharath, H.A.; Chandan, M.C.; Vinay, S.; Ramachandra, T.V. Modelling urban dynamics in rapidly urbanising Indian cities. *Egypt. J. Remote Sens. Space Sci.* **2018**, *21*, 201–210. [CrossRef]
12. Ibn, A.R.; Rudith, I.; King, S. The Contribution of Rural Urban Migration to Migrants' Economic Development in Tamale. *Res. Humanit. Soc. Sci.* **2017**, *7*, 76.
13. Selod, H.; Shilpi, F. Rural-urban migration in developing countries: Lessons from the literature. *Reg. Sci. Urban Econ.* **2021**, *91*, 103713. [CrossRef]
14. Lall, S.V.; Selod, H.; Shalizi, Z. *Rural-Urban Migration in Developing Countries: A Survey of Theoretical Predictions and Empirical Findings*; World Bank Publications: Chicago, IL, USA, 2006.
15. Manu, A.; Twumasi, Y.A.; Lu, K.S.; Coleman, T.L. Predicting urban growth of a developing country city using a statistical modeling approach. *Int. J. Geomat. Geosci.* **2015**, *5*, 603–613.
16. Seto, K.C.; Fragkias, M.; Güneralp, B.; Reilly, M.K. A Meta-Analysis of Global Urban Land Expansion. *PLoS ONE* **2011**, *6*, e23777. [CrossRef] [PubMed]
17. Rossi, J.P.; Dobigny, G. Urban Landscape Structure of a Fast-Growing African City: The Case of Niamey (Niger). *Urban Sci.* **2019**, *3*, 63. [CrossRef]
18. Srivastava, A.; Kumari, N.; Maza, M. Hydrological Response to Agricultural Land Use Heterogeneity Using Variable Infiltration Capacity Model. *Water Resour. Manag.* **2020**, *34*, 3779–3794. [CrossRef]
19. Bhattacharya, R.K.; Das Chatterjee, N.; Das, K. Land use and Land Cover change and its resultant erosion susceptible level: An appraisal using RUSLE and Logistic Regression in a tropical plateau basin of West Bengal, India. *Environ. Dev. Sustain.* **2021**, *23*, 1411–1446. [CrossRef]
20. Watson, K.E.; Gardiner, K.M.; Singleton, J.A. The impact of extreme heat events on hospital admissions to the Royal Hobart Hospital. *J. Public Health* **2020**, *42*, 333–339. [CrossRef]
21. Wald, A.; Demorest, S. Race to Beat the Heat: Climate Change Impacts Physical Activity. *J. Nurse Pract.* **2022**, *18*, 388–394. [CrossRef]
22. Hussain, S.; Lu, L.; Mubeen, M.; Nasim, W.; Karuppannan, S.; Fahad, S.; Tariq, A.; Mousa, B.G.; Mumtaz, F.; Aslam, M. Spatiotemporal Variation in Land Use Land Cover in the Response to Local Climate Change Using Multispectral Remote Sensing Data. *Land* **2022**, *11*, 595. [CrossRef]
23. Fu, P.; Weng, Q. A time series analysis of urbanization induced land use and land cover change and its impact on land surface temperature with Landsat imagery. *Remote Sens. Environ.* **2016**, *175*, 205–214. [CrossRef]
24. Li, H.; Wang, C.; Zhong, C.; Zhang, Z.; Liu, Q. Mapping Typical Urban LULC from Landsat Imagery without Training Samples or Self-Defined Parameters. *Remote Sens.* **2017**, *9*, 700. [CrossRef]
25. Derdouri, A.; Wang, R.; Murayama, Y.; Osaragi, T. Understanding the links between LULC changes and sushi in cities: Insights from two-decadal studies (2001–2020). *Remote Sens.* **2021**, *13*, 3654. [CrossRef]
26. OECD. Land Cover Monitoring 2011. Available online: http://oe.cd/land-cover (accessed on 9 November 2022).
27. Liu, X.; Li, X.; Chen, Y.; Tan, Z.; Li, S.; Ai, B. A new landscape index for quantifying urban expansion using multi-temporal remotely sensed data. *Landsc Ecol.* **2010**, *25*, 671–682. [CrossRef]
28. Mishra, G.K.; Deshmukh, A.M. Urban Sprawl in the context of proximity factors using Shannon's Entropy Index and fractal dimensions: A case of Lucknow. *J. Spat. Sci.* **2024**, *69*, 1–27. [CrossRef]

29. Rahaman, M.; Dutta, S.; Sahana, M.; Das, D.N. Analysing urban sprawl and spatial expansion of Kolkata urban agglomeration using geospatial approach. In *Applications and Challenges of Geospatial Technology: Potential Future Trends*; Springer: Cham, Switzerland, 2018; pp. 205–221.
30. Diksha; Kumar, A. Analysing urban sprawl and land consumption patterns in major capital cities in the Himalayan region using geoinformatics. *Appl. Geogr.* **2017**, *89*, 112–123. [CrossRef]
31. Dhanaraj, K.; Angadi, D.P. Urban expansion quantification from remote sensing data for sustainable land-use planning in Mangaluru, India. *Remote Sens. Appl.* **2021**, *23*, 100602.
32. Sudhira, H.S.; Ramachandra, T.V.; Jagadish, K.S. Urban sprawl: Metrics, dynamics and modelling using GIS. *Int. J. Appl. Earth Obs. Geoinf.* **2004**, *5*, 29–39. [CrossRef]
33. Akın, A.; Erdoğan, M.A. Analysing temporal and spatial urban sprawl change of Bursa city using landscape metrics and remote sensing. *Model Earth Syst. Environ.* **2020**, *6*, 1331–1343. [CrossRef]
34. Robert, S.; Fox, D.; Boulay, G.; Grandclément, A.; Garrido, M.; Pasqualini, V.; Prévost, A.; Schleyer-Lindenmann, A.; Trémélo, M.-L. A framework to analyse urban sprawl in the French Mediterranean coastal zone. *Reg. Environ. Chang.* **2019**, *19*, 559–572. [CrossRef]
35. Africa's Fastest Growing Cities 2020–2035 | Statista. Available online: https://www.statista.com/statistics/1234653/africa-s-fastest-growing-cities/ (accessed on 4 November 2024).
36. Leslie, R.C.C. Zinder, Point de Chute des Réfugiés Face à Boko Haram. Le Monde, 17 February 2015. Available online: https://www.lemonde.fr/afrique/video/2015/02/17/niger-zinder-point-de-chute-des-refugies-face-a-boko-haram_4578250_3212.html (accessed on 5 August 2024).
37. Zinder Population. World Population Review. 2024. Available online: https://worldpopulationreview.com/world-cities/zinder-population (accessed on 31 July 2024).
38. Khan, A.; Sudheer, M. Machine learning-based monitoring and modeling for spatio-temporal urban growth of Islamabad. *Egyptian J. Remote Sens. Space Sci.* **2022**, *25*, 541–550. [CrossRef]
39. Rokni, K. Investigating the Impact of Pan Sharpening on the Accuracy of Land Cover Mapping in Landsat Oli Imagery. *GeCar* **2023**, *49*, 12–18. [CrossRef]
40. Mushore, T.D.; Mutanga, O.; Odindi, J.; Sadza, V.; Dube, T. Pansharpened landsat 8 thermal-infrared data for improved Land Surface Temperature characterization in a heterogeneous urban landscape. *Remote Sens. Appl.* **2022**, *26*, 100728. [CrossRef]
41. Lin, C.; Wu, C.C.; Tsogt, K.; Ouyang, Y.C.; Chang, C.I. Effects of atmospheric correction and pansharpening on LULC classification accuracy using WorldView-2 imagery. *Inf. Process. Agric.* **2015**, *2*, 25–36. [CrossRef]
42. Breiman, L. Random Forests. *Mach. Learn.* **2001**, *45*, 5–32. [CrossRef]
43. Ali, J.; Khan, R.; Ahmad, N.; Maqsood, I. Random Forests and Decision Trees. *Int. J. Comput. Sci. Issues* **2012**, *9*, 272.
44. Rodriguez-Galiano, V.F.; Ghimire, B.; Rogan, J.; Chica-Olmo, M.; Rigol-Sanchez, J.P. An assessment of the effectiveness of a random forest classifier for land-cover classification. *ISPRS J. Photogramm. Remote Sens.* **2012**, *67*, 93–104. [CrossRef]
45. Talukdar, S.; Singha, P.; Mahato, S.; Shahfahad; Pal, S.; Liou, Y.A.; Rahman, A. Land-use land-cover classification by machine learning classifiers for satellite observations—A review. *Remote Sens.* **2020**, *12*, 1135. [CrossRef]
46. Albertini, C.; Gioia, A.; Iacobellis, V.; Petropoulos, G.P.; Manfreda, S. Assessing multi-source random forest classification and robustness of predictor variables in flooded areas mapping. *Remote Sens. Appl.* **2024**, *35*, 101239. [CrossRef]
47. Abdi, A.M. Land cover and land use classification performance of machine learning algorithms in a boreal landscape using Sentinel-2 data. *GIsci Remote Sens.* **2019**, *57*, 1–20. [CrossRef]
48. Pradhan, B.; Al-sharif, A.A.A.; Abdullahi, S. Urban Sprawl Assessment. In *Spatial Modeling and Assessment of Urban Form—Analysis of Urban Growth: From Sprawl to Compact Using Geospatial Data*; Springer: Cham, Switzerland, 2017; pp. 61–92.
49. Acheampong, R.A.; Agyemang, F.S.K.; Abdul-Fatawu, M. Quantifying the spatio-temporal patterns of settlement growth in a metropolitan region of Ghana. *GeoJournal* **2017**, *82*, 823–840. [CrossRef]
50. Wei, G.; He, B.J.; Sun, P.; Liu, Y.; Li, R.; Ouyang, X.; Luo, K.; Li, S. Evolutionary trends of urban expansion and its sustainable development: Evidence from 80 representative cities in the belt and road initiative region. *Cities* **2023**, *138*, 104353. [CrossRef]
51. Ren, P.; Gan, S.; Yuan, X.; Zong, H.; Xie, X. Spatial Expansion and Sprawl Quantitative Analysis of Mountain City Built-Up Area. *Commun. Comput. Inf. Sci.* **2013**, *398*, 166–176.
52. Sapena, M.; Ruiz, L.A. Analysis of urban development by means of multi-temporal fragmentation metrics from LULC data. *Int. Arch. Photogramm. Remote Sens. Spat. Inf. Sci.* **2015**, *XL-7/W3*, 1411–1418. [CrossRef]
53. Crawford, C.J.; Roy, D.P.; Arab, S.; Barnes, C.; Vermote, E.; Hulley, G.; Gerace, A.; Choate, M.; Engebreston, C.; Micijevic, E.; et al. The 50-year Landsat collection 2 archive. *Sci. Remote Sens.* **2023**, *8*, 100103. [CrossRef]
54. Mosammam, H.M.; Nia, J.T.; Khani, H.; Teymouri, A.; Kazemi, M. Monitoring land use change and measuring urban sprawl based on its spatial forms: The case of Qom city. *Egypt. J. Remote Sens. Space Sci.* **2017**, *20*, 103–116.
55. AlQadhi, S.; Mallick, J.; Talukdar, S.; Bindajam, A.A.; Shohan, A.A.A.; Shahfahad. Quantification of urban sprawl for past-to-future in Abha City, Saudi Arabia. *CMES Comput. Model. Eng. Sci.* **2021**, *129*, 755–786. [CrossRef]
56. Illiassou, A.S.; Boubacar, M.M.; Abou Soufianou, S.; Ali, M.; Mahamane, S. Dynamics of a third world city: Case of Niamey, Niger. *J. Geogr. Reg. Plan.* **2015**, *8*, 120–130.
57. Institut National de la Statistique du Niger. Rapport «Agriculture et Conditions de vie des Ménages. Available online: https://www.stat-niger.org/?publication_recente=rapport-agriculture-et-conditions-de-vie-des-menages (accessed on 11 July 2024).

58. PDC. *Plan de Developpement Communal (PDC) 3ème Arrondissement de la ville de Zinder*; PDC: Essex, UK, 2015.
59. Fonds International de Développement Agricole. Programme Spécial pour le Niger (PSN). Available online: https://www.ifad.org/en/w/projects/1100000441 (accessed on 11 July 2024).
60. Doulay, K.; Diouf, A.; Sadda, A.S.; Yakubu, I.B. Landuse/landcover change process in a tropical semi-arid zone: Case of two rural communes (Chadakori and Saé-Saboua) in Maradi region, Republic of Niger. *Landsc. Environ.* **2019**, *13*, 1–12.
61. Das, S.; Angadi, D.P. Land use land cover change detection and monitoring of urban growth using remote sensing and GIS techniques: A micro-level study. *GeoJournal* **2021**, *87*, 2101–2123. [CrossRef]
62. Huang, Q.; Liu, Y. The Coupling between Urban Expansion and Population Growth: An Analysis of Urban Agglomerations in China (2005–2020). *Sustainability* **2021**, *13*, 7250. [CrossRef]
63. Banai, R. Urban sprawl: Definitions, data, methods of measurement, and environmental consequences. *J. Sustain. Educ.* **2014**, *7*, 1–15.
64. Ismael, H.M. Urban form study: The sprawling city—Review of methods of studying urban sprawl. *GeoJournal* **2021**, *86*, 1785–1796. [CrossRef]
65. Chettry, V. A Critical Review of Urban Sprawl Studies. *J. Geovisualiz. Spat. Anal.* **2023**, *7*, 28. [CrossRef]
66. Sun, C.; Wu, Z.F.; Lv, Z.Q.; Yao, N.; Wei, J.B. Quantifying different types of urban growth and the change dynamic in Guangzhou using multi-temporal remote sensing data. *Int. J. Appl. Earth Obs. Geoinf.* **2013**, *21*, 409–417. [CrossRef]
67. Wilson, E.H.; Hurd, J.D.; Civco, D.L.; Prisloe, M.P.; Arnold, C. Development of a geospatial model to quantify, describe and map urban growth. *Remote Sens. Environ.* **2003**, *86*, 275–285. [CrossRef]
68. Forman, R.T.T. Some general principles of landscape and regional ecology. *Landsc. Ecol.* **1995**, *10*, 133–142. [CrossRef]
69. Jun, H.J.; Kim, D.; Kim, J.H.; Heo, J.P. Detection of infill development and contributing factors using deep learning and multilevel modeling. *Cities* **2024**, *150*, 105019. [CrossRef]
70. Heimlich, R.E.; Anderson, W.D. *Development at the Urban Fringe and Beyond: Impacts on Agriculture and Rural Land*; Dedication; Economic Research Service (ERS) of the U.S. Department of Agriculture (USDA): Washington, DC, USA, 2001.
71. Abdoulaye, A. Croissance urbaine et dysfonctionnements: Cas de l'arrondissement communal Zinder III. *Ann. De L'université De Parakou* **2019**, *2*.
72. Wu, D.; Zheng, L.; Wang, Y.; Gong, J.; Li, J.; Chen, Q. Urban expansion patterns and their driving forces analysis: A comparison between Chengdu-Chongqing and Middle Reaches of Yangtze River urban agglomerations. *Environ. Monit Assess* **2023**, *195*, 1121. [CrossRef]
73. Zhu, X.X.; Tuia, D.; Mou, L.; Xia, G.S.; Zhang, L.; Xu, F.; Fraundorfer, F. Deep learning in remote sensing: A review. *IEEE Geosci. Remote Sens. Mag.* **2017**, *5*, 8–36. [CrossRef]
74. Carranza-García, M.; García-Gutiérrez, J.; Riquelme, J.C. A Framework for Evaluating Land Use and Land Cover Classification Using Convolutional Neural Networks. *Remote Sens.* **2019**, *11*, 274. [CrossRef]

Disclaimer/Publisher's Note: The statements, opinions and data contained in all publications are solely those of the individual author(s) and contributor(s) and not of MDPI and/or the editor(s). MDPI and/or the editor(s) disclaim responsibility for any injury to people or property resulting from any ideas, methods, instructions or products referred to in the content.